ELSEVIER

Composites: Part B 31 (2000) 511–526

composites
Part B: engineering

www.elsevier.com/locate/compositesb

Cement reinforced with short carbon fibers: a multifunctional material

D.D.L. Chung*

Composite Materials Research Laboratory, State University of New York at Buffalo, Buffalo, NY 14260-4400, USA

Received 1 November 1999; accepted 8 December 1999

Abstract

This is a review of cement-matrix composites containing short carbon fibers. These composites exhibit attractive tensile and flexural properties, low drying shrinkage, high specific heat, low thermal conductivity, high electrical conductivity, high corrosion resistance and weak thermoelectric behavior. Moreover, they facilitate the cathodic protection of steel reinforcement in concrete, and have the ability to sense their own strain, damage and temperature. Fiber surface treatment can improve numerous properties of the composites. Conventional carbon fibers of diameter 15 μm are more effective than 0.1 μm diameter carbon filaments as a reinforcement, but are much less effective for radio wave reflection (EMI shielding). Carbon fiber composites are superior to steel fiber composites for strain sensing, but are inferior to steel fiber composites in the thermoelectric behavior.

Keywords: A. Carbon fiber; B. Mechanical properties; Cement

1. Introduction

Carbon fiber cement-matrix composites are structural materials that are gaining in importance quite rapidly due to the decrease in carbon fiber cost [1] and the increasing demand of superior structural and functional properties. These composites contain short carbon fibers, typically 5 mm in length, as the short fibers can be used as an admixture in concrete (whereas continuous fibers cannot be simply added to the concrete mix) and short fibers are less expensive than continuous fibers. However, due to the weak bond between carbon fiber and the cement matrix, continuous fibers [2–4] are much more effective than short fibers in reinforcing concrete. Surface treatment of carbon fiber (e.g. by heating [5] or by using ozone [6,7], silane [8], SiO_2 particles [9] or hot NaOH solution [10]) is useful for improving the bond between fiber and matrix, thereby improving the properties of the composite. In the case of surface treatment by ozone or silane, the improved bond is due to the enhanced wettability by water. Admixtures such as latex [6,11] methylcellulose [6] and silica fume [12] also help the bond.

The effect of carbon fiber addition on the properties of concrete increases with fiber volume fraction [13], unless the fiber volume fraction is so high that the air void content becomes excessively high [14]. (The air void content increases with fiber content and air voids tend to have a negative effect on many properties, such as the compressive strength.) In addition, the workability of the mix decreases with fiber content [13]. Moreover, the cost increases with fiber content. Therefore, a rather low volume fraction of fibers is desirable. A fiber content as low as 0.2 vol.% is effective [15], although fiber contents exceeding 1 vol.% are more common [16,20]. The required fiber content increases with the particle size of the aggregate, as the flexural strength decreases with increasing particle size [21].

Effective use of the carbon fibers in concrete requires dispersion of the fibers in the mix. The dispersion is enhanced by using silica fume (a fine particulate) as an admixture [14,22–24]. A typical silica fume content is 15% by weight of cement [14]. The silica fume is typically used along with a small amount (0.4% by weight of cement) of methylcellulose for helping the dispersion of the fibers and the workability of the mix [14]. Latex (typically 15–20% by weight of cement) is much less effective than silica fume for helping the fiber dispersion, but it enhances the workability, flexural strength, flexural toughness, impact resistance, frost resistance and acid resistance [14,25,26]. The ease of dispersion increases with decreasing fiber length [24].

The improved structural properties rendered by carbon fiber addition pertain to the increased tensile and flexible strengths, the increased tensile ductility and flexural toughness, the enhanced impact resistance, the reduced drying shrinkage and the improved freeze–thaw durability [13–15,17–25,27–38].

* Tel.: + 1-716-645-2593; fax: + 1-716-645-3875.
E-mail address: ddlchung@acsu.buffalo.edu (D.D.L. Chung).

1359-8368/00/$ - see front matter
PII: S1359-8368(99)00071-2

Table 1
Properties of carbon fibers

Filament diameter	15 ± 3 μm
Tensile strength	690 MPa
Tensile modulus	48 GPa
Elongation at break	1.4%
Electrical resistivity	3.0×10^{-3} Ω cm
Specific gravity	1.6 g cm^{-3}
Carbon content	98 wt.%

The tensile and flexural strengths decrease with increasing specimen size, such that the size effect becomes larger as the fiber length increases [39]. The low drying shrinkage is valuable for large structures and for use in repair [40,41] and in joining bricks in a brick structure [42,43]. The functional properties rendered by carbon fiber addition pertain to the strain sensing ability [7,44–57] (for smart structures), the temperature sensing ability [58–61], the damage sensing ability [44,48,62–64], the thermoelectric behavior [59–61], the thermal insulation ability [65–67] (to save energy for buildings), the electrical conduction ability [68–77] (to facilitate cathodic protection of embedded steel and to provide electrical grounding or connection), and the radio wave reflection/absorption ability [78–83] (for electromagnetic interference or EMI shielding, for lateral guidance in automatic highways, and for television image transmission).

In relation to the structural properties, carbon fibers compete with glass, polymer and steel fibers [18,27–29,32,36–38,84]. Carbon fibers (isotropic pitch based) [1,84] are advantageous in their superior ability to increase the tensile strength of concrete, even though the tensile strength, modulus and ductility of the isotropic pitch based carbon fibers are low compared to most other fibers. Carbon fibers are also advantageous in the relative chemical inertness [85]. PAN-based carbon fibers are also used [17,19,22,33], although they are more commonly used as continuous fibers than short fibers. Carbon-coated glass fibers [86,87] and submicron diameter carbon filaments [76–78] are even less commonly used, although the former is attractive for the low cost of glass fibers and the latter is attractive for its high radio wave reflectivity (which results from the skin effect). C-shaped carbon fibers are more effective for strengthening than round carbon fibers [88], but their relatively large diameter makes them less attractive. Carbon fibers can be used in concrete together with steel fibers, as the addition of short carbon fibers to steel fiber reinforced mortar increases the fracture toughness of the interfacial zone between steel fiber and the cement matrix [89]. Carbon fibers can also be used in concrete together with steel bars [90,91], or together with carbon fiber reinforced polymer rods [92].

Table 2
Tensile strength (MPa) of cement pastes with and without fibers (A: cement + water + water reducing agent + silica fume, A^+: A + methylcellulose + defoamer, A^+F: A^+ + as-received fibers, A^+O: A^+ + O_3-treated fibers, A^+K: A^+ + dichromate-treated fibers, A^+S: A^+ + silane-treated fibers)

Formulation	As-received silica fume	Silane-treated silica fume
A	1.53 ± 0.06	2.04 ± 0.06
A^+	1.66 ± 0.07	2.25 ± 0.09
A^+F	2.00 ± 0.09	2.50 ± 0.11
A^+O	2.25 ± 0.07	2.67 ± 0.09
A^+K	2.32 ± 0.08	2.85 ± 0.11
A^+S	2.47 ± 0.11	3.12 ± 0.12

Table 3
Tensile strength (GPa) of cement pastes with and without fibers (A: cement + water + water reducing agent + silica fume, A^+: A + methylcellulose + defoamer, A^+F: A^+ + as-received fibers, A^+O: A^+ + O_3-treated fibers, A^+K: A^+ + dichromate-treated fibers, A^+S: A^+ + silane-treated fibers)

Formulation	As-received silica fume	Silane-treated silica fume
A	10.2 ± 0.7	11.5 ± 0.6
A^+	9.3 ± 0.5	10.7 ± 0.4
A^+F	10.9 ± 0.3	12.9 ± 0.7
A^+O	11.9 ± 0.3	13.1 ± 0.6
A^+K	12.7 ± 0.4	14.3 ± 0.4
A^+S	13.3 ± 0.5	15.2 ± 0.8

In relation to most functional properties, carbon fibers are exceptional compared to the other fiber types. Carbon fibers are electrically conducting, in contrast to glass and polymer fibers, which are not conducting. Steel fibers are conducting, but their typical diameter (≥60 μm) is much larger than the diameter of a typical carbon fiber (15 μm). The combination of electrical conductivity and small diameter makes carbon fibers superior to the other fiber types in the area of strain sensing and electrical conduction. However, carbon fibers are inferior to steel fibers for providing thermoelectric composites, due to the high electron concentration in steel and the low hole concentration in carbon.

Although carbon fibers are thermally conducting, addition of carbon fibers to concrete lowers the thermal conductivity [65], thus allowing applications related to thermal insulation. This effect of carbon fiber addition is due to the increase in air void content. The electrical conductivity of carbon fibers is higher than that of the cement matrix by about eight orders of magnitude, whereas the thermal conductivity of carbon fibers is higher than that of the cement matrix by only one or two orders of magnitude. As a result, the electrical conductivity is increased upon carbon fiber addition in spite of the increase in air void content, but the thermal conductivity is decreased upon fiber addition.

The use of pressure after casting [93], and extrusion [94,95] can result in composites with superior microstructure and properties. Moreover, extrusion improves the shapability [95].

This paper is a review of short carbon fiber reinforced cement-matrix composites, including concrete (with fine and coarse aggregates), mortar (with fine aggregate and no

Table 4
Tensile ductility (%) of cement pastes with and without fibers (A: cement + water + water reducing agent + silica fume, A^+: A + methylcellulose + defoamer, A^+F: A^+ + as-received fibers, A^+O: A^+ + O_3-treated fibers, A^+K: A^+ + dichromate-treated fibers, A^+S: A^+ + silane-treated fibers)

Formulation	As-received silica fume	Silane-treated silica fume
A	0.020 ± 0.0004	0.020 ± 0.0004
A^+	0.023 ± 0.0004	0.021 ± 0.0004
A^+F	0.025 ± 0.0003	0.024 ± 0.0004
A^+O	0.026 ± 0.0003	0.027 ± 0.0004
A^+K	0.028 ± 0.0003	0.030 ± 0.0004
A^+S	0.031 ± 0.0004	0.034 ± 0.0004

coarse aggregate) and cement paste. Previous reviews are noted [96–101].

Table 1 shows the properties of the isotropic-pitch-based carbon fibers (15 μm in diameter, nominally 5 mm long) used by the author in the cement-matrix composites described below for the purpose of illustration.

2. Structural behavior

The properties relevant to the structural behavior of cement-matrix composites containing short carbon fibers are given in this section.

Tables 2 and 3 show the tensile strength and modulus, respectively, of 12 types of cement pastes. The strength is slightly increased by the addition of methylcellulose and defoamer, but the modulus is slightly decreased by the addition of methylcellulose and defoamer. However, both strength and modulus are increased by the addition of fibers. The effectiveness of the fibers in increasing strength and modulus increases in the following order: as-received fibers, O_3-treated fibers, dichromate-treated fibers, and silane-treated fibers. This trend applies whether the silica fume is as-received or silane-treated. For any of the formulations, silane-treated silica fume gives substantially higher strength and modulus than as-received silica fume. The highest tensile strength and modulus are exhibited by cement paste with silane-treated silica fume and silane-treated fibers. The strength is 56% higher and the modulus is 39% higher than those of the cement paste with as-received silica fume and as-received fibers. The strength is 26% higher and the modulus is 14% higher than those of the cement paste with as-received silica fume and silane-treated fibers. Hence, silane treatments of silica fume and of fibers are about equally valuable in providing strengthening.

Table 5
Air void content (%, ±0.12) of cement pastes with and without fibers (A: cement + water + water reducing agent + silica fume, A^+: A + methylcellulose + defoamer, A^+F: A^+ + as-received fibers, A^+O: A^+ + O_3-treated fibers, A^+K: A^+ + dichromate-treated fibers, A^+S: A^+ + silane-treated fibers)

Formulation	As-received silica fume	Silane-treated silica fume
A	3.73	3.26
A^+	3.42	3.01
A^+F	5.32	4.89
A^+O	5.07	4.65
A^+K	5.01	4.49
A^+S	4.85	4.16

Table 4 shows the tensile ductility. It is slightly increased by the addition of methylcellulose and defoamer, and is further increased by the further addition of fibers. The effectiveness of the fibers in increasing the ductility also increases in the above order. This trend applies whether the silica fume is as-received or silane-treated. For any of the formulations involving surface treated fibers, silane-treated silica fume gives higher ductility than as-received silica fume. The highest ductility is exhibited by cement paste with silane-treated silica fume and silane-treated fibers. The ductility is 39% higher than that of the cement paste with as-received silica fume and as-received fibers. It is 14% higher than that of the cement paste with as-received silica fume and silane-treated fibers.

Table 5 shows the air void content. It is decreased by the addition of methylcellulose and defoamer, but is increased by the further addition of fibers, whether the fibers have been surface treated or not. Among the formulations with fibers, the air void content decreases in the following order: as-received fibers, O_3-treated fibers, dichromate-treated fibers and silane-treated fibers. This trend applies whether the silica fume is as-received or silane-treated. For any of the formulations (including those without fibers), silane-treated silica fume gives lower air void content than as-received silica fume.

Tables 6–8 give the dynamic flexural properties of 12 types of cement pastes. Six of the types have as-received silica fume; the other six have silane-treated silica fume.

The loss tangent (Table 6) is increased slightly by the addition of methylcellulose. Further addition of carbon fibers decreases the loss tangent. The loss tangent decreases in the following order: as-received fibers, ozone-treated fibers, dichromate-treated fibers and silane-treated fibers, at least for the case of as-received silica fume at 0.2 Hz.

The storage modulus (Table 7) is decreased by the addition of methylcellulose. Further addition of carbon fibers increases the storage modulus, such that the modulus increases in the order: as-received fibers, ozone-treated fibers, dichromate-treated fibers and silane-treated fibers. These trends apply whether the silica fume is as-received or silane-treated, and whether the frequency is 0.2, 1.0 or 2.0 Hz.

The loss modulus (Table 8, product of loss tangent and storage modulus) is increased by the addition of methylcellulose, except for the case of the paste with silane-treated silica fume at 0.2 Hz. Further addition of carbon fibers increases the loss modulus very slightly, if at all.

Table 9 gives the drying shrinkage strain of ten types of cement paste as a function of curing age. The drying shrinkage is decreased by the addition of carbon fibers, such that it decreases in the following order: as-received

Table 6
Loss tangent (tan δ, ± 0.002) of cement pastes (A: cement + water + water reducing agent + silica fume, A^+: A + methylcellulose + defoamer, A^+F: A^+ + as-received fibers, A^+O: A^+ + O_3-treated fibers, A^+K: A^+ + dichromate-treated fibers, A^+S: A^+ + silane-treated fibers)

Formulation	With as-received silica fume			With silane-treated silica fume		
	0.2 Hz	1.0 Hz	2.0 Hz	0.2 Hz	1.0 Hz	2.0 Hz
A	0.082	0.030	$< 10^{-4}$	0.087	0.032	$< 10^{-4}$
A^+	0.102	0.045	$< 10^{-4}$	0.093	0.040	$< 10^{-4}$
A^+F	0.089	0.033	$< 10^{-4}$	0.084	0.034	$< 10^{-4}$
A^+O	0.085	0.043	$< 10^{-4}$	0.084	0.032	$< 10^{-4}$
A^+K	0.079	0.039	$< 10^{-4}$	0.086	0.035	$< 10^{-4}$
A^+S	0.076	0.036	$< 10^{-4}$	0.083	0.033	$< 10^{-4}$

Table 7
Storage modulus (GPa, ± 0.03) of cement pastes (A: cement + water + water reducing agent + silica fume, A^+: A + methylcellulose + defoamer, A^+F: A^+ + as-received fibers, A^+O: A^+ + O_3-treated fibers, A^+K: A^+ + dichromate-treated fibers, A^+S: A^+ + silane-treated fibers)

Formulation	With as-received silica fume			With silane-treated silica fume		
	0.2 Hz	1.0 Hz	2.0 Hz	0.2 Hz	1.0 Hz	2.0 Hz
A	12.71	12.14	11.93	16.75	16.21	15.95
A^+	11.52	10.61	10.27	15.11	14.73	14.24
A^+F	13.26	13.75	13.83	17.44	17.92	18.23
A^+O	14.14	14.46	14.72	18.92	19.36	19.57
A^+K	15.42	16.15	16.53	19.33	19.85	20.23
A^+S	17.24	17.67	15.95	21.34	21.65	21.97

Table 8
Loss modulus (GPa, ± 0.03) of cement pastes (A: cement + water + water reducing agent + silica fume, A^+: A + methylcellulose + defoamer, A^+F: A^+ + as-received fibers, A^+O: A^+ + O_3-treated fibers, A^+K: A^+ + dichromate-treated fibers, A^+S: A^+ + silane-treated fibers)

Formulation	With as-received silica fume			With silane-treated silica fume		
	0.2 Hz	1.0 Hz	2.0 Hz	0.2 Hz	1.0 Hz	2.0 Hz
A	1.04	0.39	$< 10^{-3}$	1.46	0.52	$< 10^{-3}$
A^+	1.18	0.48	$< 10^{-3}$	1.41	0.59	$< 10^{-3}$
A^+F	1.18	0.45	$< 10^{-3}$	1.47	0.61	$< 10^{-3}$
A^+O	1.20	0.62	$< 10^{-3}$	1.59	0.62	$< 10^{-3}$
A^+K	1.22	0.63	$< 10^{-3}$	1.66	0.70	$< 10^{-3}$
A^+S	1.31	0.63	$< 10^{-3}$	1.77	0.71	$< 10^{-3}$

Table 9
Drying shrinkage strain (10^{-4}, ± 0.015) different curing ages (B: cement + water + water reducing agent + silica fume + methylcellulose + defoamer, BF: B + as-received fibers, BO: B + O_3-treated fibers, BK: B + dichromate-treated fibers, BS: B + silane-treated fibers)

Formulation	With as-received silica fume				With silane-treated silica fume			
	1 day	4 days	8 days	19 days	1 day	4 days	8 days	19 days
B	1.128	3.021	3.722	4.365	1.013	2.879	3.623	4.146
BF	0.832	2.417	3.045	3.412	0.775	2.246	2.810	3.113
BO	0.825	2.355	3.022	3.373	0.764	2.235	2.793	3.014
BK	0.819	2.321	3.019	3.372	0.763	2.232	2.790	3.010
BS	0.812	2.316	2.976	3.220	0.752	2.118	2.724	2.954

Table 10
Specific heat (J/g K, ±0.001) of cement pastes. The value for plain cement paste (with cement and water only) is 0.736 J/g K (A: cement + water + water reducing agent + silica fume, A^+: A + methylcellulose + defoamer, A^+F: A^+ + as-received fibers, A^+O: A^+ + O_3-treated fibers, A^+K: A^+ + dichromate-treated fibers, A^+S: A^+ + silane-treated fibers)

Formulation	As-received silica fume	Silane-treated silica fume
A	0.782	0.788
A^+	0.793	0.803
A^+F	0.804	0.807
A^+O	0.809	0.813
A^+K	0.812	0.816
A^+S	0.819	0.823

Table 11
Thermal diffusivity (mm^2/s, ±0.03) of cement pastes. The value for plain cement paste (with cement and water only) is 0.36 mm^2/s (A: cement + water + water reducing agent + silica fume, A^+: A + methylcellulose + defoamer, A^+F: A^+ + as-received fibers, A^+O: A^+ + O_3-treated fibers, A^+K: A^+ + dichromate-treated fibers, A^+S: A^+ + silane-treated fibers)

Formulation	As-received silica fume	Silane-treated silica fume
A	0.26	0.24
A^+	0.25	0.22
A^+F	0.27	0.26
A^+O	0.29	0.27
A^+K	0.29	0.27
A^+S	0.25	0.23

fibers, ozone-treated fibers, dichromate-treated fibers and silane-treated fibers. This trend applies for any curing age, whether the silica fume is as-received or silane-treated. The drying shrinkage is decreased by the use of silane-treated silica fume in place of as-received silica fume, whether fibers are present or not. The drying shrinkage strain at 28 days is decreased by 5% when fibers are absent and silane-treated silica fume is used in place of as-received silica fume. When silane-treated fibers are present, it is decreased by 10% when silane-treated silica fume is used in place of as-received silica fume. By adding silane-treated fibers to the paste with as-received silica fume, the shrinkage at 28 days is decreased by 25%. By adding silane-treated fibers to the paste with silane-treated silica fume, the shrinkage at 28 days is decreased by 28%. By adding silane-treated fibers and replacing as-received silica fume by silane-treated silica fume, the shrinkage at 28 days is decreased by 32%.

3. Non-structural behavior

3.1. Thermal behavior

Table 10 shows the specific heat of cement pastes. The specific heat is significantly increased by the addition of silica fume. It is further increased by the further addition of methylcellulose and defoamer. It is still further increased by the still further addition of carbon fibers. The effectiveness of the fibers in increasing the specific heat increases in the following order: as-received fibers, O_3-treated fibers, dichromate-treated fibers and silane-treated fibers. This trend applies whether the silica fume is as-received or silane-treated. For any of the formulations, silane-treated silica fume gives higher specific heat than as-received silica fume. The highest specific heat is exhibited by the cement paste with silane-treated silica fume and silane-treated fibers. The specific heat is 12% higher than that of plain cement paste, 5% higher than that of the cement paste with as-received silica fume and as-received fibers, and 0.5% higher than that of the cement paste with as-received silica fume and silane-treated fibers. Hence, silane treatment of fibers is more valuable than that of silica fume for increasing the specific heat.

Table 11 shows the thermal diffusivity of cement pastes. The thermal diffusivity is significantly decreased by the addition of silica fume. The further addition of methylcellulose and defoamer or the still further addition of fibers has relatively little effect on the thermal diffusivity. Surface treatment of the fibers by ozone or dichromate slightly increases the thermal diffusivity, whereas surface treatment of the fibers by silane slightly decreases the thermal diffusivity. These trends apply whether the silica fume is as-received or silane-treated. For any of the formulations, silane-treated silica fume gives slightly lower (or essentially the same) thermal diffusivity than as-received silica fume. Silane treatments of silica fume and of fibers are about equally effective for lowering the thermal diffusivity.

Table 12 shows the density of cement pastes. The density is significantly decreased by the addition of silica fume. It is further decreased slightly by the further addition of methylcellulose and defoamer. It is still further decreased by the still further addition of fibers. The effectiveness of the fibers in decreasing the density decreases in the following order: as-received fibers, O_3-treated fibers, dichromate-treated fibers and silane-treated fibers. This trend applies whether the silica fume is as-received or silane-treated. For any of the formulations, silane-treated silica fume gives slightly higher (or essentially the same) specific heat than as-received silica fume. Silane treatment of fibers is more valuable than that of silica fume for increasing the density.

Table 13 shows the thermal conductivity. It is significantly decreased by the addition of silica fume. The further addition of methylcellulose and defoamer or the still further addition of fibers has little effect on the density. Surface treatment of the fibers by ozone or dichromate slightly increases the thermal conductivity, whereas surface treatment of the fibers by silane has negligible effect. These trends apply whether the silica fume is as-received or silane-treated. For any of the formulations, silane-treated silica fume gives slightly lower (or essentially the same) thermal conductivity as as-received silica fume. Silane

Table 12
Density (g/cm^3, ±0.02) of cement pastes. The value for plain cement paste (with cement and water only) is 2.01 g/cm^3 (A: cement + water + water reducing agent + silica fume, A^+: A + methylcellulose + defoamer, A^+F: A^+ + as-received fibers, A^+O: A^+ + O_3-treated fibers, A^+K: A^+ + dichromate-treated fibers, A^+S: A^+ + silane-treated fibers)

Formulation	As-received silica fume	Silane-treated silica fume
A	1.72	1.73
A^+	1.69	1.70
A^+F	1.62	1.64
A^+O	1.64	1.65
A^+K	1.65	1.66
A^+S	1.66	1.68

treatments of silica fume and of fibers contribute comparably to reducing the thermal conductivity.

3.2. Electrical behavior

Fig. 1 gives the volume electrical resistivity of composites at 7 days of curing. The resistivity decreases much with increasing fiber volume fraction, whether a second filler (silica fume or sand) is present or not. When sand is absent, the addition of silica fume decreases the resistivity at all carbon fiber volume fractions except the highest volume fraction of 4.24%; the decrease is most significant at the lowest fiber volume fraction of 0.53%. When sand is present, the addition of silica fume similarly decreases the resistivity, such that the decrease is most significant at fiber volume fractions below 1%. When silica fume is absent, the addition of sand decreases the resistivity only when the fiber volume fraction is below about 0.5%; at high fiber volume fractions, the addition of sand even increases the resistivity due to the porosity induced by the sand. Thus, the addition of a second filler (silica fume or sand) that is essentially nonconducting decreases the resistivity of the composite only at low volume fractions of the carbon fibers and the maximum fiber volume fraction for the resistivity to decrease is larger when the particle size of the filler is smaller. The resistivity decrease is attributed to the improved fiber dispersion due to the presence of the second filler. Consistent with the improved fiber dispersion is the increased flexural toughness and strength due to the presence of the second filler.

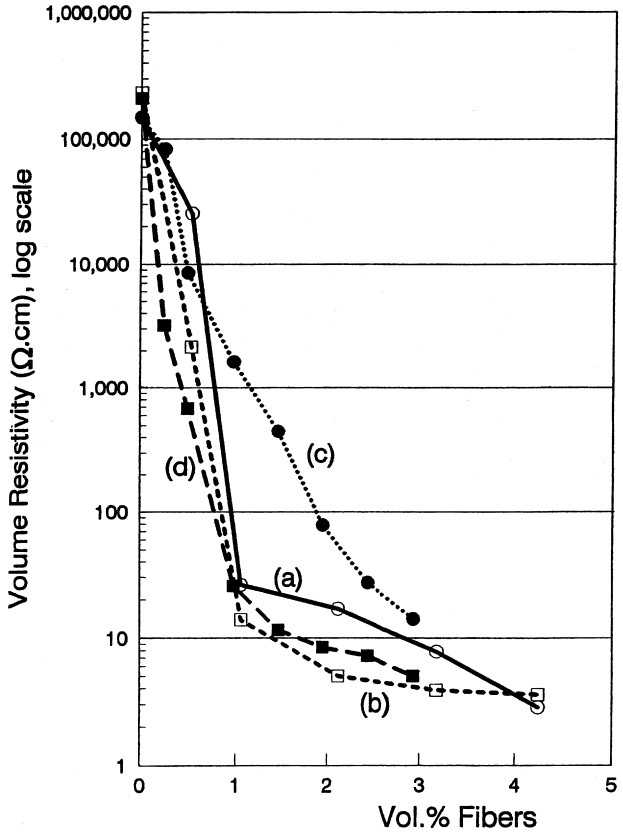

Fig. 1. Variation of the volume electrical resistivity with carbon fiber volume fraction: (a) without sand, with methylcellulose, without silica fume; (b) without sand, with methylcellulose, with silica fume; (c) with sand, with methylcellulose, without silica fume; (d) with sand, with methylcellulose, with silica fume.

Table 13
Thermal conductivity (W/m K, ±0.03) of cement pastes. The value for plain cement paste (with cement and water only) is 0.53 W/m K (A: cement + water + water reducing agent + silica fume, A^+: A + methylcellulose + defoamer, A^+F: A^+ + as-received fibers, A^+O: A^+ + O_3-treated fibers, A^+K: A^+ + dichromate-treated fibers, A^+S: A^+ + silane-treated fibers)

Formulation	As-received silica fume	Silane-treated silica fume
A	0.35	0.33
A^+	0.34	0.30
A^+F	0.35	0.34
A^+O	0.38	0.36
A^+K	0.39	0.37
A^+S	0.34	0.32

Fig. 2 shows the fractional increase in conductivity (reciprocal of resistivity) due to the fibers alone. At a given fiber volume fraction, the fractional increase is higher when silica fume is present, whether sand is present or not. At fiber volume fractions above 1%, the use of silica fume but no sand gives the highest fractional increase, while the use of sand but no silica fume gives the lowest fractional increase. At fiber volume fractions below 1%, the use of both sand and silica fume gives the highest fractional increase, while the use of no sand nor silica fume gives the lowest fractional increase.

Fig. 3 shows the measured conductivity as a fraction of the calculated value obtained from the Rule of Mixtures by assuming that the fibers were continuous and parallel along the axis of the conductivity measurement. This fraction provides an indication of the degree of fiber dispersion. At a given fiber volume fraction, it is higher when silica fume is present, whether sand is present or not. When sand is absent, the use of silica fume does not affect the percolation threshold volume fraction (1%), but increases the fibers' effectiveness. When sand is present, the use of silica fume

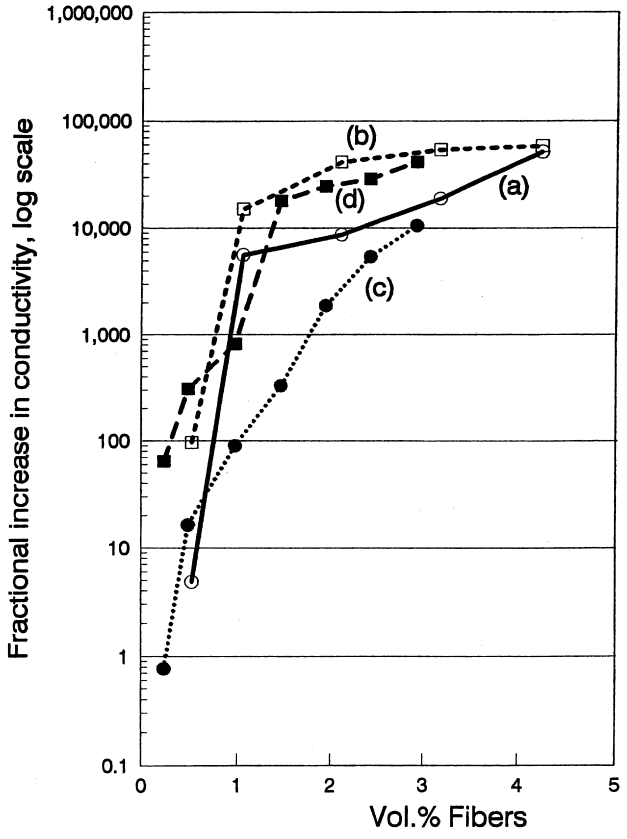

Fig. 2. Variation with the carbon fiber volume fraction of the fractional increase in volume electrical conductivity due to the carbon fibers alone: (a) without sand, with methylcellulose, without silica fume; (b) without sand, with methylcellulose, with silica fume; (c) with sand, with methylcellulose, without silica fume; (d) with sand, with methylcellulose, with silica fume.

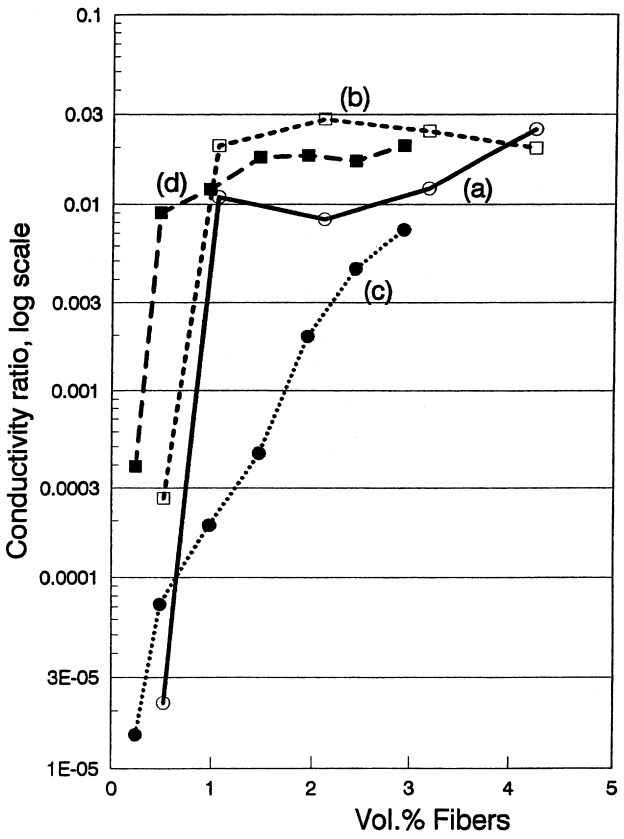

Fig. 3. Variation with the carbon fiber volume fraction of the ratio of the measured volume electrical conductivity to the calculated value obtained from the Rule of Mixtures by assuming that the fibers were continuous and unidirectional along the axis of conductivity measurement. The matrix conductivity used in the calculation was the measured conductivity for the case without fibers but containing the corresponding additives, i.e. either methylcellulose or methylcellulose + silica fume: (a) without sand, with methylcellulose, without silica fume; (b) without sand, with methylcellulose, with silica fume; (c) with sand, with methylcellulose, without silica fume; (d) with sand, with methylcellulose, with silica fume.

greatly diminishes the percolation threshold volume fraction. On the other hand, the addition of sand without silica fume greatly increases the threshold.

The use of both silica fume and sand results in an electrical resistivity of $3.19 \times 10^3\ \Omega$ cm at a carbon fiber volume fraction of just 0.24 vol.%. This is an outstandingly low resistivity value compared to those of polymer-matrix composites with discontinuous conducting fillers at similar volume fractions.

3.3. Radio wave reflectivity

Due to the electrical conductivity of carbon fibers, the addition of carbon fibers to cement significantly increases the ability of the composite to reflect radio waves, thus allowing EMI shielding and lateral guidance in automatic highways. However, due to the skin effect (the phenomenon in which electromagnetic radiation at a high frequency, such as 1 GHz, penetrates only the near surface region of a conductor), discontinuous carbon filaments of 0.1 μm diameter, as made from carbonaceous gases by catalytic growth, are much more effective for radio wave reflection than conventional pitch-based carbon fibers of diameter 15 μm [78–81]. However, the 0.1 μm diameter filaments are less effective than the 15 μm diameter fibers as a reinforcement.

The cement-matrix composites are more effective than corresponding polymer-matrix composites for radio wave reflection, due to the slight conductivity of the cement matrix and the insulating nature of the polymer matrix. The conductivity of the cement matrix allows some electrical connectivity of the filler units, even when the filler concentration is below the percolation threshold [79].

3.4. Cathodic protection of steel reinforcement in concrete

Cathodic protection is one of the most common and effective methods for corrosion control of steel reinforced concrete. This method involves the application of a voltage so as to force electrons to go to the steel reinforcing bar (rebar), thereby making the steel a cathode. As the steel rebar is embedded in concrete, the electrons need to go through the concrete in order to reach the rebar. However,

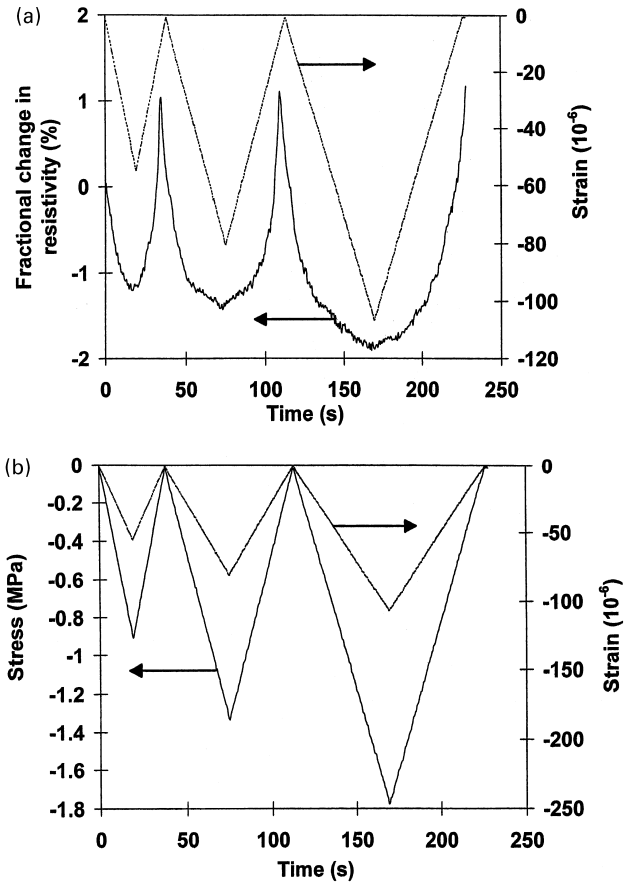

Fig. 4. Variation of the fractional change in volume electrical resistivity with time (a), of the stress with time (b), and of the strain (negative for compressive strain) with time (a,b) during dynamic compressive loading at increasing stress amplitudes within the elastic regime for carbon-fiber latex cement paste at 28 days of curing.

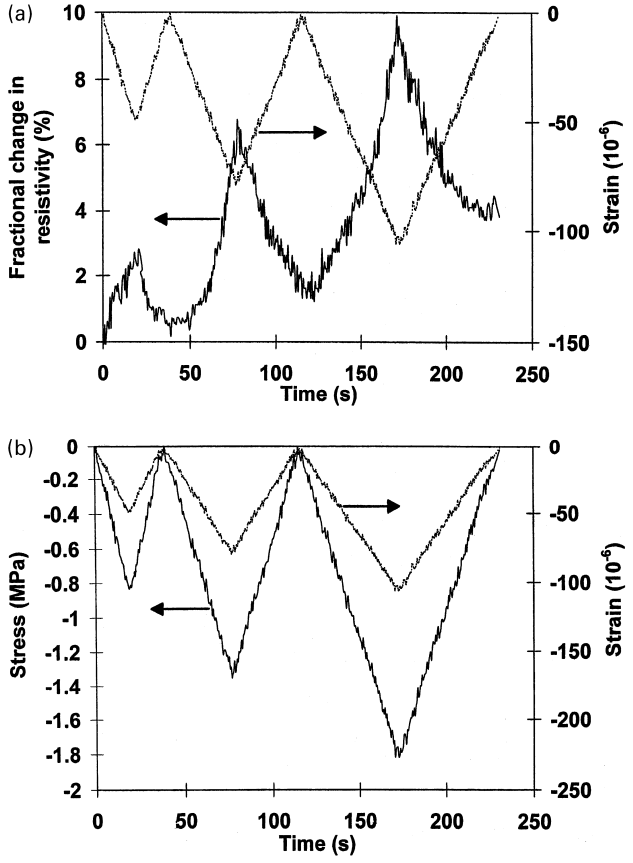

Fig. 5. Variation of the fractional change in volume electrical resistivity with time (a), of the stress with time (b), and of the strain (negative for compressive strain) with time (a,b) during dynamic compressive loading at increasing stress amplitudes within the elastic regime for carbon-fiber latex cement paste at 7 days of curing.

concrete is not very conducting electrically. The use of carbon fiber reinforced concrete for embedding the rebar to be cathodically protected facilitates cathodic protection, as the short carbon fibers enhance the conductivity of the concrete.

For directing electrons to the steel reinforced concrete to be cathodically protected, an electrical contact is needed on the concrete. The electrical contact is electrically connected to the voltage supply. One of the choices of an electrical contact material is zinc, which is a coating deposited on the concrete by thermal spraying. It has a very low volume resistivity (thus requiring no metal mesh embedment), but it suffers from poor wear and corrosion resistance, the tendency to oxidize, high thermal expansion coefficient, and high material and processing costs. Another choice is a conductor filled polymer [102], which can be applied as a coating without heating, but it suffers from poor wear resistance, high thermal expansion coefficient and high material cost. Yet another choice is a metal (e.g. titanium) strip or wire embedded at one end in cement mortar, which is in the form of a coating on the steel reinforced concrete. The use of carbon fiber reinforced mortar for this coating facilitates cathodic protection, as it is advantageous to enhance the conductivity of this coating.

Due to the decrease in volume electrical resistivity associated with carbon fiber addition (0.35 vol.%) to concrete (embedding steel rebar), concrete containing carbon fibers and silica fume reduces by 18% the driving voltage required for cathodic protection compared to plain concrete, and by 28% compared to concrete with silica fume. Due to the decrease in resistivity associated with carbon fiber addition (1.1 vol.%) to mortar, overlay (embedding titanium wires for electrical contacts to steel reinforced concrete) in the form of mortar containing carbon fibers and latex reduces by 10% the driving voltage required for cathodic protection, compared to plain mortar overlay. In spite of the low resistivity of mortar overlay with carbon fibers, cathodic protection requires multiple metal electrical contacts embedded in the mortar at a spacing of 11 cm or less.

3.5. Strain and damage sensing

Fig. 4(a) shows the fractional change in resistivity along the stress axis as well as the strain during repeated compressive loading at an increasing stress amplitude for

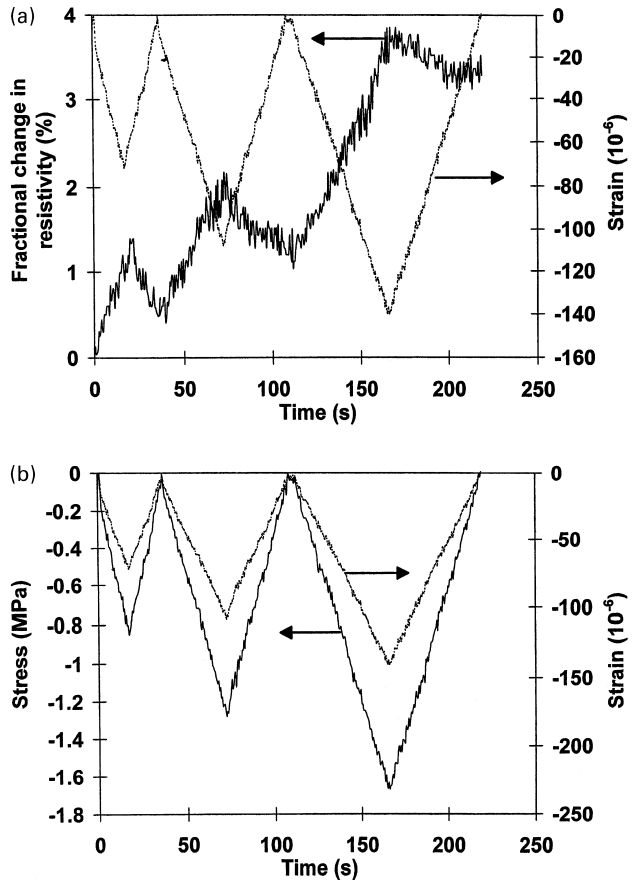

Fig. 6. Variation of the fractional change in volume electrical resistivity with time (a), of the stress with time (b), and of the strain (negative for compressive strain) with time (a,b) during dynamic compressive loading at increasing stress amplitudes within the elastic regime for latex cement paste at 7 days of curing.

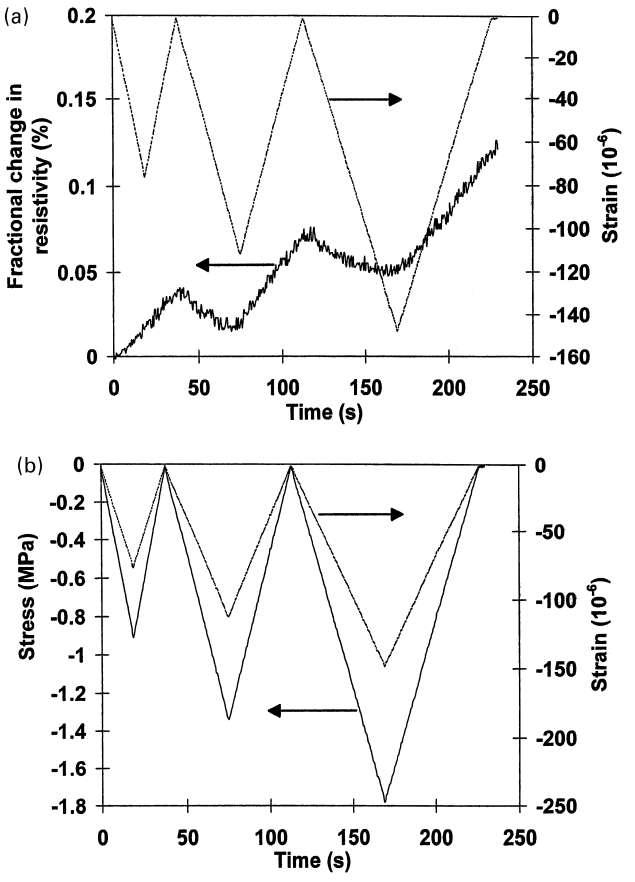

Fig. 7. Variation of the fractional change in volume electrical resistivity with time (a), of the stress with time (b), and of the strain (negative for compressive strain) with time (a,b) during dynamic compressive loading at increasing stress amplitudes within the elastic regime for latex cement paste at 28 days of curing.

carbon-fiber latex cement paste at 28 days of curing. Fig. 4(b) shows the corresponding variation of stress and strain during the repeated loading. The strain varies linearly with the stress up to the highest stress amplitude (Fig. 4(b)). The strain returns to zero at the end of each cycle of loading. The resistivity decreases upon loading in every cycle (due to fiber push-in) and increases upon unloading in every cycle (due to fiber pull-out). The resistivity has a net increase after the first cycle, due to very minor damage. Little further damage occurs in subsequent cycles, as shown by the resistivity after unloading not increasing much after the first cycle. The greater the strain amplitude, the more is the resistivity decrease during loading, although the resistivity and strain are not linearly related. The effects of Fig. 4 were similarly observed in carbon-fiber silica-fume cement paste at 28 days of curing.

Fig. 5 gives the corresponding plots for carbon-fiber latex cement paste at 7 days of curing. Comparison of Figs. 4 and 5 shows that (i) the resistivity increases upon loading at 7 days (Fig. 5), but decreases upon loading at 28 days (Fig. 4), (ii) the resistivity increase upon loading at 7 days is not totally reversible, whereas the resistivity decrease upon loading at 28 days is totally reversible, and (iii) the fractional increase in resistivity upon loading is up to 10% at 7 days, but the fractional decrease in resistivity upon loading is only up to 2% at 28 days, though R_0 is similar at 7 and 28 days. The effects in Fig. 5 were similarly observed in carbon-fiber silica-fume cement paste at 7 days. The changeover from the 7 day behavior to the 28 day behavior occurs between 7 and 14 days.

Although the fractional change in resistivity upon loading is larger at 7 days (Fig. 5) than at 28 days (Fig. 4) for carbon-fiber latex cement paste, the greater reversibility upon unloading and the less noise in the resistivity variation at 28 days makes the behavior at 28 days more attractive than that at 7 days for use in resistance-based strain sensing. In practice, concrete is used in a fully cured state (exceeding 28 days of curing). Therefore, the behavior at 28 days is practically more important than that at 7 days. Nevertheless, the behavior at 7 days is of fundamental interest.

Comparison of Figs. 6 and 5 (both at 7 days) shows that the effects are qualitatively similar with fibers (Fig. 5) and without fibers (Fig. 6), though (i) the fractional change in resistivity is larger in the presence of fibers, and (ii) the

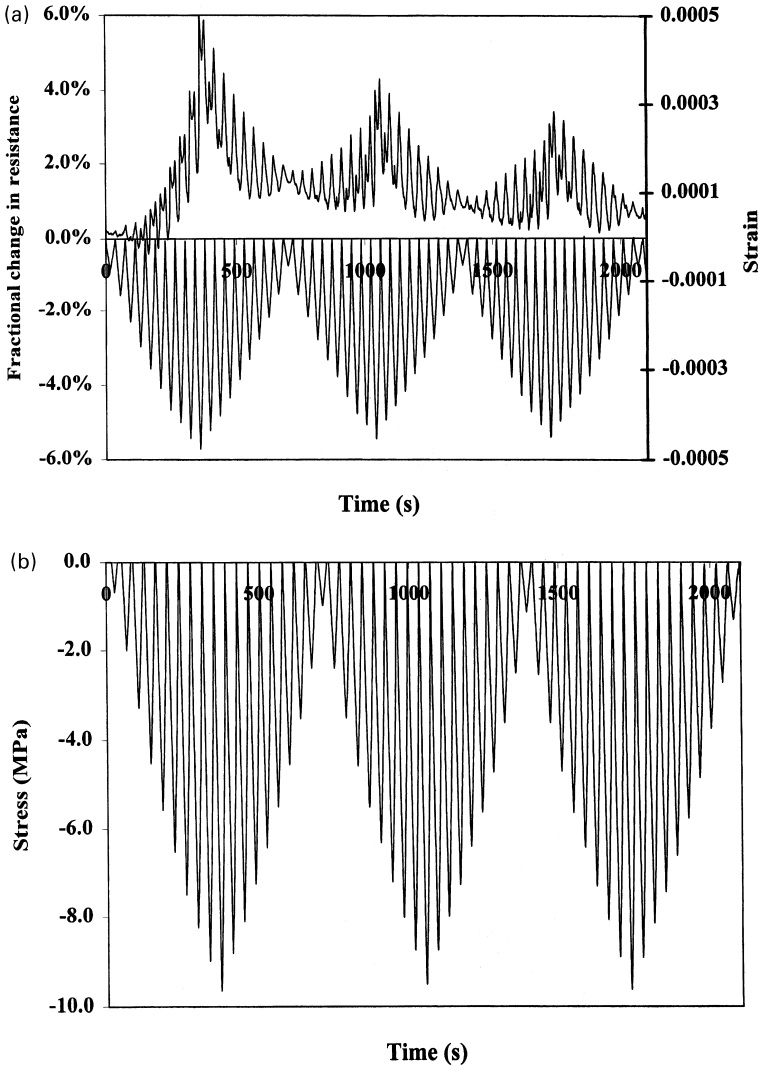

Fig. 8. Fractional change in resistance (a), strain (a) and stress (b) during repeated compressive loading at increasing and decreasing stress amplitudes, the highest of which was 60% of the compressive strength, for carbon fiber concrete at 28 days of curing.

resistivity increase upon loading is more reversible in the presence of fibers. Thus, the origins of the effects in Figs. 6 and 5 are basically similar, though the presence of fibers, which are electrically conductive, in Fig. 5 adds to the types of defects that are generated upon loading and the fiber-related defects make the resistivity changes more pronounced and more reversible.

Comparison of Figs. 7 and 4 (both at 28 days) shows that the effects are qualitatively and quantitatively different between latex cement paste (Fig. 7) and carbon-fiber latex cement paste (Fig. 4). In the presence of carbon fibers, the resistivity decreases reversibly upon loading; in the absence of fibers, the resistivity mainly increases upon unloading.

Figs. 4–7 show that the effect of carbon fibers on the variation of the resistivity with strain is more drastic at 28 days than at 7 days.

Fig. 8 shows the fractional change in resistance, strain and stress during repeated compressive loading at increasing and decreasing stress amplitudes for carbon fiber concrete at 28 days of curing. The highest stress amplitude is 60% of the compressive strength. A group of cycles in which the stress amplitude increases cycle by cycle and then decreases cycle by cycle back to the initial low stress amplitude is hereby referred to as a group. Fig. 8 shows the results for three groups. The strain returns to zero at the end of each cycle for any of the stress amplitudes, indicating elastic behavior. The resistance decreases upon loading in each cycle, as in Fig. 4. An extra peak at the maximum stress of a cycle grows as the stress amplitude increases, resulting in two peaks per cycle. The original peak (strain induced) occurs at zero stress, while the extra peak (damage induced) occurs at the maximum stress. Hence, during loading from zero stress within a cycle, the resistance drops and then increases sharply, reaching the maximum resistance of the extra peak at the maximum stress of the cycle. Upon subsequent unloading, the resistance decreases and then increases

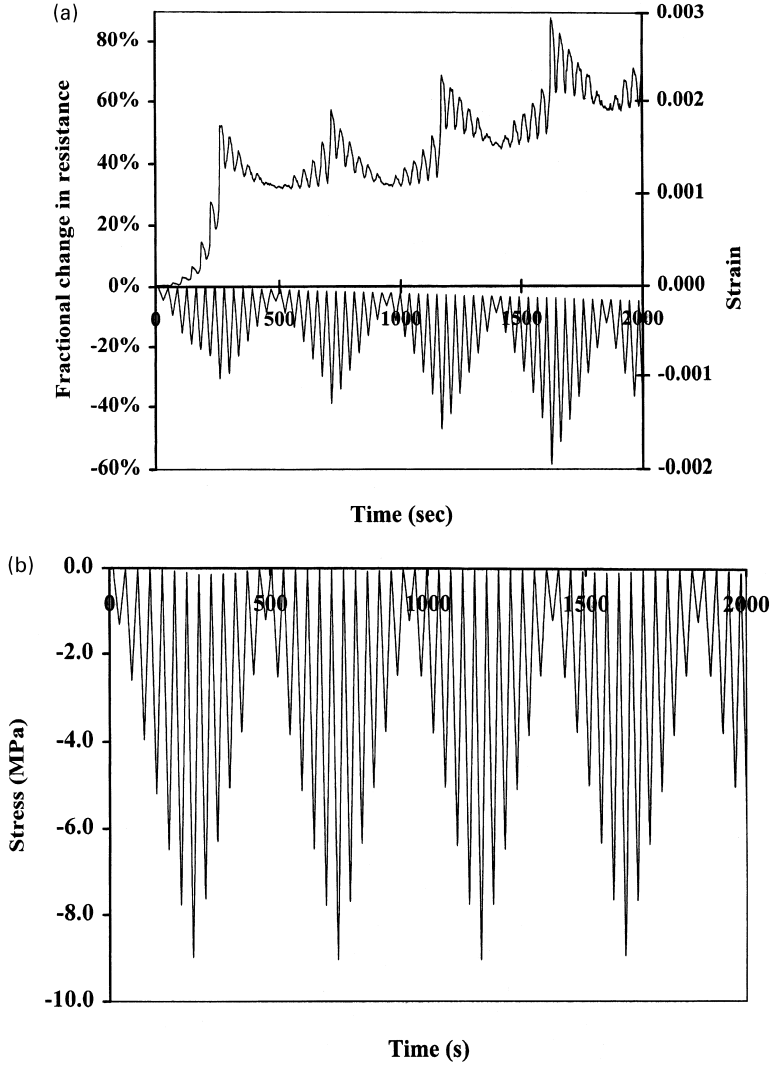

Fig. 9. Fractional change in resistance (a), strain (a) and stress (b) during repeated compressive loading at increasing and decreasing stress amplitudes, the highest of which was >90% of the compressive strength, for carbon fiber concrete at 28 days of curing.

as unloading continues, reaching the maximum resistance of the original peak at zero stress. In the part of this group where the stress amplitude decreases cycle by cycle, the extra peak diminishes and disappears, leaving the original peak as the sole peak. In the part of the second group where the stress amplitude increases cycle by cycle, the original peak (peak at zero stress) is the sole peak, except that the extra peak (peak at the maximum stress) returns in a minor way (more minor than in the first group) as the stress amplitude increases. The extra peak grows as the stress amplitude increases, but, in the part of the second group in which the stress amplitude decreases cycle by cycle, it quickly diminishes and vanishes, as in the first group. Within each group, the amplitude of resistance variation increases as the stress amplitude increases and decreases as the stress amplitude subsequently decreases.

The greater the stress amplitude, the larger and the less reversible is the damage-induced resistance increase (the extra peak). If the stress amplitude has been experienced before, the damage-induced resistance increase (the extra peak) is small, as shown by comparing the result of the second group with that of the first group (Fig. 8), unless the extent of damage is large (Fig. 9 for a highest stress amplitude of >90% the compressive strength). When the damage is extensive (as shown by a modulus decrease), damage-induced resistance increase occurs in every cycle, even at a decreasing stress amplitude, and it can overshadow the strain-induced resistance decrease (Fig. 9). Hence, the damage-induced resistance increase occurs mainly during loading (even within the elastic regime), particularly at a stress above that in prior cycles, unless the stress amplitude is high and/or damage is extensive.

At a high stress amplitude, the damage-induced resistance increase cycle by cycle as the stress amplitude increases causes the baseline resistance to increase irreversibly (Fig. 9). The baseline resistance in the regime of major damage (with a decrease in modulus) provides a measure of the extent of damage (i.e. condition monitoring). This measure

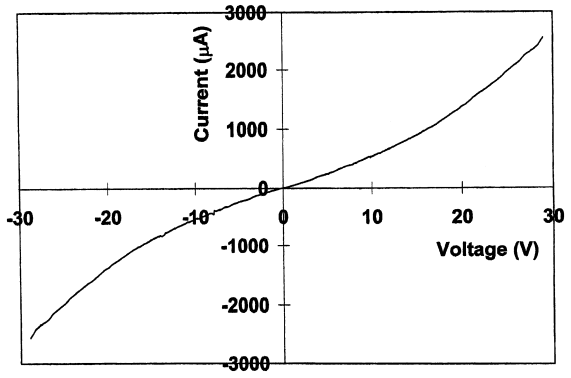

Fig. 10. Current–voltage characteristic of carbon-fiber silica-fume cement paste at 38°C during stepped heating.

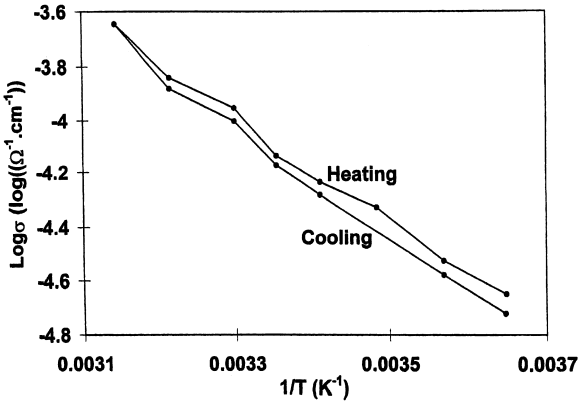

Fig. 12. Arrhenius plot of log electrical conductivity vs. reciprocal absolute temperature for carbon-fiber silica-fume cement paste.

works in the loaded or unloaded state. In contrast, the measure using the damage-induced resistance increase (Fig. 8) works only during stress increase and indicates the occurrence of damage (whether minor or major) as well as the extent of damage.

The damage causing the partially reversible damage-induced resistance increase is probably mainly associated with partially reversible degradation of the fiber–matrix interface. The reversibility rules out fiber fracture as the main type of damage, especially at a low stress amplitude. At a high stress amplitude, the extent of reversibility diminishes and fiber fracture may contribute to cause the damage. Fiber fracture can occur during the opening of a crack that is bridged by a fiber. The fiber–matrix interface degradation may be associated with slight fiber pull-out upon slight crack opening for cracks that are bridged by fibers. The severity of the damage-induced resistance increase supports the involvement of the fibers in the damage mechanism, as the fibers are much more conducting than the matrix.

3.6. Temperature sensing through the thermistor effect

A thermistor is a thermometric device consisting of a material (typically a semiconductor, but in this case a cement paste) whose electrical resistivity decreases with rise in temperature.

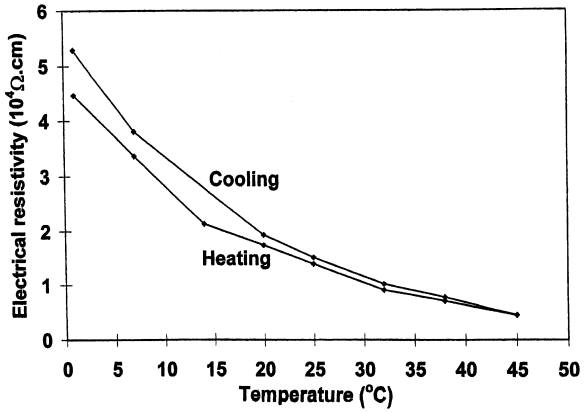

Fig. 11. Plot of volume electrical resistivity vs. temperature during heating and cooling for carbon-fiber silica-fume cement paste.

Fig. 10 shows the current–voltage characteristic of carbon-fiber (0.5% by weight of cement) silica-fume (15% by weight of cement) cement paste at 38°C during stepped heating. The characteristic is linear below 5 V and deviates positively from linearity beyond 5 V. The resistivity is obtained from the slope of the linear portion. The voltage at which the characteristic starts to deviate from linearity is referred to as the critical voltage.

Fig. 11 shows a plot of the resistivity vs. temperature during heating and cooling for carbon-fiber silica-fume cement paste. The resistivity decreases upon heating and the effect is quite reversible upon cooling. That the resistivity is slightly increased after a heating–cooling cycle is probably due to thermal degradation of the material. Fig. 12 shows the Arrhenius plot of log conductivity (conductivity = 1/resistivity) vs. reciprocal absolute temperature. The slope of the plot gives the activation energy, which is 0.390 ± 0.014 and 0.412 ± 0.017 eV during heating and cooling, respectively.

Results similar to those of carbon-fiber silica-fume cement paste were obtained with carbon-fiber (0.5% by weight of cement) latex (20% by weight of cement) cement paste, silica-fume cement paste, latex cement paste and plain cement paste. However, for all these four types of cement paste, (i) the resistivity is higher by about an order of magnitude, and (ii) the activation energy is lower by about an order of magnitude, as shown in Table 14. The critical voltage is higher when fibers are absent (Table 14).

3.7. Thermoelectric behavior

The Seebeck effect is a thermoelectric effect which is the basis for thermocouples for temperature measurement. This effect involves charge carriers moving from a hot point to a cold point within a material, thereby resulting in a voltage difference between the two points. The Seebeck coefficient is the voltage difference per unit temperature difference

Table 14
Resistivity, critical voltage and activation energy of five types of cement paste

Formulation	Resistivity at 20°C (Ω cm)	Critical voltage at 20°C (V)	Activation energy (eV)	
			Heating	Cooling
Plain	$(4.87 \pm 0.37) \times 10^5$	10.80 ± 0.45	0.040 ± 0.006	0.122 ± 0.006
Silica fume	$(6.12 \pm 0.15) \times 10^5$	11.60 ± 0.37	0.035 ± 0.003	0.084 ± 0.004
Carbon fibers + silica fume	$(1.73 \pm 0.08) \times 10^4$	8.15 ± 0.34	0.390 ± 0.014	0.412 ± 0.017
Latex	$(6.99 \pm 0.12) \times 10^5$	11.80 ± 0.31	0.017 ± 0.001	0.025 ± 0.002
Carbon fibers + latex	$(9.64 \pm 0.08) \times 10^4$	8.76 ± 0.35	0.018 ± 0.001	0.027 ± 0.002

between the two points. Negative carriers (electrons) make it more positive and positive carriers (holes) make it more negative.

Eight types of cement paste were studied comparitively, namely: (i) plain cement paste (consisting of just cement and water); (ii) silica-fume cement paste (consisting of cement, water and silica fume); (iii) carbon-fiber silica-fume cement paste (consisting of cement, water, silica fume, methylcellulose, defoamer and carbon fibers in the amount of 0.5% by weight of cement); (iv) carbon-fiber silica-fume cement paste (same as (iii) except for having carbon fibers in the amount of 1.0% by weight of cement); (v) carbon-fiber silica-fume cement paste (same as (iii) except for having carbon fibers in the amount of 1.5% by weight of cement); (vi) latex cement paste (consisting of cement, water, latex and antifoam); (vii) carbon-fiber latex cement paste (consisting of cement, water, latex, antifoam and carbon fibers in the amount of 0.5% by weight of cement; and (viii) carbon-fiber latex cement paste (same as (vii) except for having carbon fibers in the amount of 1.0% by weight of cement).

Table 15 shows the Seebeck coefficient (with copper as the reference) and the absolute thermoelectric power. A negative value of the absolute thermoelectric power indicates p-type (hole) behavior; a positive value indicates n-type (electron) behavior. All types of cement paste studied are n-type except pastes (iv) and (v), which were p-type. The higher the fiber content, the less n-type (the more p-type) is the paste, whether silica fume or latex is present. Without fibers, the absolute thermoelectric power is 2 μV/°C, whether silica fume and latex are present or not. This is consistent with the similar values of the electrical conductivity for cement pastes with silica fume and with latex, but without fibers. Thus, silica fume or latex addition does not have much influence on the thermoelectric power when fibers are absent, but carbon fiber addition does by enhancing the hole conduction.

As shown in Table 15, the thermopower results obtained during heating and cooling are very close. Fig. 13 shows the variation of the Seebeck voltage vs. the temperature difference during heating and cooling for paste (iii). With fibers present, the variation is linear and essentially identical during heating and cooling. Without fibers, the variation is non-linear and hysteretic (i.e. not totally reversible upon cooling subsequent to heating). Thus, although the fiber addition does not increase the magnitude of the absolute thermoelectric power, it enhances the linearity and reversibility of the Seebeck effect. This enhancement is attributed to the increase in the contribution of holes to the electrical conduction and the association of hole conduction to conduction through the fibers.

The absolute thermoelectric power monotonically becomes less positive (more negative) as the fiber content increases through the percolation threshold, which is at a fiber content between 0.5 and 1.0% by weight of cement. The change of the absolute thermoelectric power from positive to negative values occurs at a fiber content between 0.5 and 1.0% by weight of cement when silica fume is present. This means that at this fiber content, which happens to be the percolation threshold, compensation takes place

Table 15
Seebeck coefficient (μV/°C) and absolute thermoelectric power (μV/°C) of eight types of cement paste

Cement paste	Heating		Cooling	
	Seebeck coefficient[a]	Absolute thermoelectric power	Seebeck coefficient[a]	Absolute thermoelectric power
(i) Plain	−(0.35 ± 0.03)	1.99 ± 0.03	−(0.38 ± 0.05)	1.96 ± 0.05
(ii) Silica fume	−(0.31 ± 0.02)	2.03 ± 0.02	−(0.36 ± 0.03)	1.98 ± 0.03
(iii) 0.5% fibers + silica fume	−(1.45 ± 0.09)	0.89 ± 0.09	−(1.45 ± 0.09)	0.89 ± 0.09
(iv) 1.0% fibers + silica fume	−(2.82 ± 0.11)	−0.48 ± 0.11	−(2.82 ± 0.11)	−0.48 ± 0.11
(v) 1.5% fibers + silica fume	−(3.10 ± 0.14)	−0.76 ± 0.14	−(3.10 ± 0.14)	−0.76 ± 0.14
(vi) Latex	−(0.28 ± 0.02)	2.06 ± 0.02	−(0.30 ± 0.02)	2.04 ± 0.02
(vii) 0.5% fibers + latex	−(1.20 ± 0.05)	1.14 ± 0.05	−(1.20 ± 0.05)	1.14 ± 0.05
(viii) 1.0% fibers + latex	−(2.10 ± 0.08)	0.24 ± 0.08	−(2.10 ± 0.08)	0.24 ± 0.08

[a] With copper as the reference.

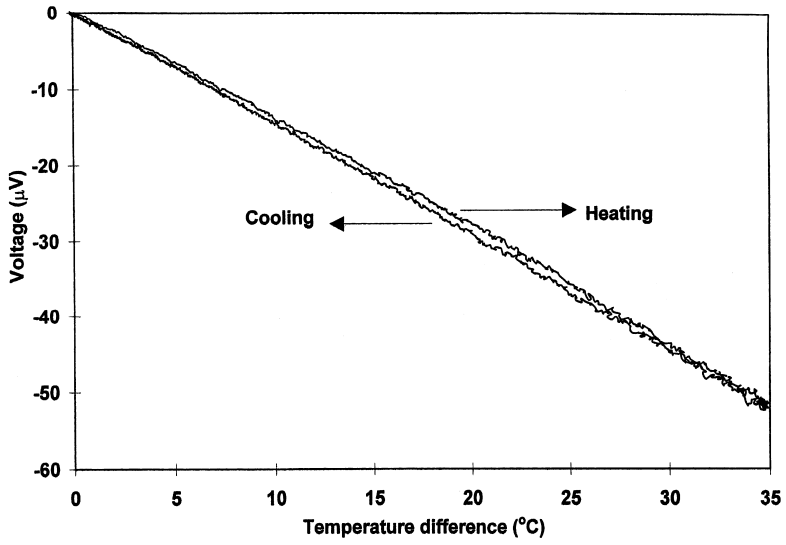

Fig. 13. Variation of the Seebeck voltage (with copper as the reference) vs. the temperature difference during heating and cooling for cement paste (iii), i.e. carbon-fiber silica-fume cement paste.

between the electron contribution from the cement matrix and the hole contribution from the fibers. It should be noted that, at any fiber content, electrons and holes contribute additively to the electrical conductivity, but subtractively to the thermopower. The correlation between the percolation threshold and change in sign of the absolute thermoelectric power is reasonable since the fibers dominate the conduction by means of holes above the percolation threshold and the cement matrix dominates the conduction by means of electrons below the percolation threshold. In the presence of latex instead of silica fume, the highest fiber content investigated was 1.0% by weight of cement and a change in sign of the absolute thermoelectric power was not observed, even though the percolation threshold is also between fiber contents of 0.5 and 1.0% by weight of cement for the case of latex. Although a change in sign of the absolute thermoelectric power was not observed for the case of latex, the absolute thermoelectric power is a very small positive value at a fiber content of 1.0% by weight of cement and the absolute thermoelectric power decreases monotonically with increasing fiber content. Based on this trend, it is highly probable that a change in sign would occur just above 1.0% by weight of cement for the case of latex. That a change in sign of the absolute thermoelectric power does not occur at the percolation threshold (but probably just above the threshold) is attributed to the low conductivity of carbon-fiber latex cement paste compared to carbon-fiber silica-fume cement paste at the same fiber content and the associated weaker hole conduction in the latex case. This is consistent with the observation that, at the same fiber content (whether 0.5 or 1.0% by weight of cement), the absolute thermoelectric power is more positive for the latex case than the silica fume case (Table 15).

The use of steel fibers instead of carbon fibers results in highly positive (up to 68 μV/°C) values of the absolute thermoelectric power, as steel fibers involve electron conduction whereas carbon fibers involve hole conduction [103]. The high values mean that the use of steel fibers gives a superior thermoelectric material then the use of carbon fibers.

3.8. Corrosion resistance

Carbon fibers decrease the corrosion resistance of steel rebar in concrete, mainly due to the decrease in the volume electrical resistivity of concrete. However, the negative effect can be compensated by adding either silica fume or latex. Silica fume is more effective than latex for improving the corrosion resistance of carbon fiber concrete. This is mainly because silica fume reduces the water absorptivity. The small increases in electrical resistivity of carbon fiber concrete after adding either silica fume or latex contribute only slightly to the effect on corrosion. Corrosion of rebar in concrete with silica fume and carbon fibers is inactive in $Ca(OH)_2$ solution, but active in NaCl solution. However, the corrosion resistance in NaCl is better than rebar in plain concrete and similar to that of rebar in latex concrete without fibers [104].

4. Conclusion

Short carbon fiber cement-matrix composites exhibit attractive tensile and flexural properties, low drying shrinkage, high specific heat, low thermal conductivity, high electrical conductivity, high corrosion resistance and weak thermoelectric behavior. Moreover, they facilitate the cathodic protection of steel reinforcement in concrete, and have the ability to sense their own strain, damage and temperature.

Acknowledgements

This work was supported in part by the National Science Foundation of USA.

References

[1] Newman JW. In: International SAMPE Symposium Exhibition, vol. 32, SAMPE, Covina, CA, 1987. p. 938–44.
[2] Furukawa S, Tsuji Y, Otani S. In: Proceedings of the 30th Japan Congress on Materials Research, Society of Materials Science, Kyoto, Japan, 1987:149–52.
[3] Saito K, Kawamura N, Kogo Y. Advanced materials: the big payoff, National SAMPE Technical Conference, Covina, CA, 1989:796–802.
[4] Wen S, Chung DDL. Cen Concr Res 1999;29(3):445–9.
[5] Sugama T, Kukacka LE, Carciello N, Stathopoulos D. Cem Concr Res 1989;19(3):355–65.
[6] Fu X, Lu W, Chung DDL. Cem Concr Res 1996;26(7):1007–12.
[7] Fu X, Lu W, Chung DDL. Carbon 1998;36(9):1337–45.
[8] Xu Y, Chung DDL. Cem Concr Res 1999;29(5):773–6.
[9] Yamada T, Yamada K, Hayashi R, Herai T. In: International SAMPE Symposium Exhibition, vol 36, SAMPE, Covina, CA, pt 1, 1991:362–71.
[10] Sugama T, Kukacka LE, Carciello N, Galen B. Cem Concr Res 1988;18(2):290–300.
[11] Larson BK, Drzal LT, Sorousian P. Composites 1990;21(3):205–15.
[12] Katz A, Li VC, Kazmer A. J Mater Civil Engng 1995;7(2):125–8.
[13] Park SB, Lee BI. Cem Concr Composites 1993;15(3):153–63.
[14] Chen P, Fu X, Chung DDL. ACI Mater J 1997;94(2):147–55.
[15] Chen P, Chung DDL. Composites 1993;24(1):33–52.
[16] Brandt AM, Kucharska L. Materials for the new millennium. In: Proceedings of Material Engineering Conference, vol. 1, ASCE, New York, NY, 1996:271–80.
[17] Toutanji HA, El-Korchi T, Katz RN, Leatherman GL. Cem Concr Res 1993;23(3):618–26.
[18] Banthia N, Sheng J. Cem Concr Composites 1996;18(4):251–69.
[19] Toutanji HA, El-Korchi T, Katz RN. Com Con Composites 1994;16(1):15–21.
[20] Akihama S, Suenaga T, Banno T. Int J Cem Composites Lightweight Concrete 1984;6(3):159–68.
[21] Kamakura M, Shirakawa K, Nakagawa K, Ohta K, Kashihara S. Sumitomo Metals 1983.
[22] Katz A, Bentur A. Cem Concr Res 1994;24(2):214–20.
[23] Ohama Y, Amano M. In: Proceedings of the 27th Japan Congress on Materials Research, Society of Material Science, Kyoto, Japan, 1983:187–91.
[24] Ohama Y, Amano M, Endo M. Concrete Int: Design Construction 1985;7(3):58–62.
[25] Zayat K, Bayasi Z. ACI Mater J 1996;93(2):178–81.
[26] Soroushian P, Aouadi F, Nagi M. ACI Mater J 1991;88(1):11–18.
[27] Mobasher B, Li CY. ACI Mater J 1996;93(3):284–92.
[28] Banthia N, Moncef A, Chokri K, Sheng J. Can J Civil Engng 1994;21(6):999–1011.
[29] Mobasher M, Li CY. Infrastructure: new materials and methods of repair. In: Proceedings of Material Engineering Conference, vol. 804, ASCE, New York, NY, 1994:551–8.
[30] Soroushian P, Nagi M, Hsu J. ACI Mater J 1992;89(3):267–76.
[31] Soroushian P. Construction Specifier 1990;43(12):102–8.
[32] Lal AK. Batiment Int/Building Res Practice 1990;18(3):153–61.
[33] Park SB, Lee BI, Lim YS. Cem Concr Res 1991;21(4):589–600.
[34] Park SB, Lee BI. High Temperatures—High Pressures 1990;22(6):663–70.
[35] Soroushian P, Nagi M, Okwuegbu A. ACI Mater J 1992;89(5):491–4.
[36] Pigeon M, Azzabi M, Pleau R. Cem Concr Res 1996;26(8):1163–70.
[37] Banthia N, Chokri K, Ohama Y, Mindess S. Adv Cem Based Mater 1994;1(3):131–41.
[38] Banthia N, Yan C, Sakai K. Com Concr Composites 1998;20(5):393–404.
[39] Urano T, Murakami K, Mitsui Y, Sakai H. Composites: Part A 1996;27(3):183–7.
[40] Ali A, Ambalavanan R. Indian Concrete J 0000;72(12):669–75.
[41] Chen P, Fu X, Chung DDL. Cem Concr Res 1995;25(3):491–6.
[42] Zhu M, Chung DDL. Cem Concr Res 1997;27(12):1829–39.
[43] Zhu M, Wetherhold RC, Chung DDL. Cem Concr Res 1997;27(3):437–51.
[44] Chen P, Chung DDL. Smart Mater Struct 1993;2:22–30.
[45] Chen P, Chung DDL. Composites Part B 1996;27:11–23.
[46] Chen P, Chung DDL. J Am Ceram Soc 1995;78(3):816–8.
[47] Chung DDL. Smart Mater Struct 1995;4:59–61.
[48] Chen P, Chung DDL. ACI Mater J 1996;93(4):341–50.
[49] Fu X, Chung DDL. Cem Concr Res 1996;26(1):15–20.
[50] Fu X, Ma E, Chung DDL, Anderson WA. Cem Concr Res 1997;27(6):845–52.
[51] Fu X, Chung DDL. Cem Concr Res 1997;27(9):1313–8.
[52] Fu X, Lu W, Chung DDL. Cem Concr Res 1998;28(2):183–7.
[53] Shi Z, Chung DDL. Cem Concr Res 1999;29(3):435–9.
[54] Mao Q, Zhao B, Sheng D, Li Z. J Wuhan U Tech, Mater Sci Ed 1996;11(3):41–45.
[55] Mao Q, Zhao B, Shen D, Li Z. Fuhe Cailiao Xuebao/Acta Materiae Compositae Sinica 1996;13(4):8–11.
[56] Sun M, Mao Q, Li Z. J Wuhan U Tech, Mater Sci Ed 1998;13(4):58–61.
[57] Zhao B, Li Z, Wu D. J Wuhan U Tech, Mater Sci Ed 1995;10(4):52–6.
[58] Wen S, Chung DDL. Cem Concr Res 1999;29(6):961–5.
[59] Sun M, Li Z, Mao Q, Shen D. Cem Concr Res 1998;28(4):549–54.
[60] Sun M, Li Z, Mao Q, Shen D. Cem Concr Res 1998;28(12):1707–12.
[61] Wen S, Chung DDL. Cem Concr Res 1999;29(12):1989–93.
[62] Bontea D, Chung DDL, Lee GC. Cem Concr Res 2000 (in press).
[63] Wen S, Chung DDL. Cem Concr Res 2000 (in press).
[64] Lee J, Batson G. Materials for the new millennium. In: Proceedings of the 4th Material Engineering Conference, vol. 2, ASCE, New York, NY, 1996:887–96.
[65] Fu X, Chung DDL. ACI Mater J 1999;96(4):455–61.
[66] Xu Y, Chung DDL. Cem Concr Res 1999;29(7):1117–21.
[67] Shinozaki Y. Adv. Mater.: looking ahead to the 21st century. In: Proceedings of the 22nd National SAMPE Technical Conference, vol. 22, SAMPE, Covina, CA, 1990:986–97.
[68] Fu X, Chung DDL. Cem Concr Res 1995;25(4):689–94.
[69] Hou J, Chung DDL. Cem Concr Res 1997;27(5):649–56.
[70] Clemena GG. Materials Performance 1988;27(3):19–25.
[71] Brousseau RJ, Pye GB. ACI Mater J 1997;94(4):306–10.
[72] Chen P, Chung DDL. Smart Mater Struct 1993;2:181–8.
[73] Chen P, Chung DDL. J Electron Mater 1995;24(1):47–51.
[74] Wang X, Wang Y, Jin Z. Fuhe Cailiao Xuebao/Acta Materiae Compositae Sinica 1998;15(3):75–80.
[75] Banthia N, Djeridane S, Pigeon M. Cem Concr Res 1992;22(5):804–14.
[76] Xie P, Gu P, Beaudoin JJ. J Mater Sci 1996;31(15):4093–7.
[77] Shui Z, Li J, Huang F, Yang D. J Wuhan U Tech, Mater Sci Ed 1995;10(4):37–41.
[78] Fu X, Chung DDL. Cem Concr Res 1998;28(6):795–801.
[79] Fu X, Chung DDL. Carbon 1998;36(4):459–62.
[80] Fu X, Chung DDL. Cem Concr Res 1996;26(10):1467–72.
[81] Fu X, Chung DDL. Cem Concr Res 1997;27(2):314.
[82] Fujiwara T, Ujie H. Tohoku Kogyo Daigaku Kiyo 1: Rikogakuhen 1987;7:179–88.
[83] Shimizu Y, Nishikata A, Maruyama N, Sugiyama A. Terebijon

Gakkaishi/J Inst Television Engineers of Japan 1986;40(8):780–5.
[84] Chen P, Chung DDL. ACI Mater J 1996;93(2):129–33.
[85] Uomoto T, Katsuki F. Doboku Gakkai Rombun-Hokokushu/Proc Japan Soc Civil Engineers, vol. 490, pt 5–23, 1994–1995:167–74.
[86] Huang CM, Zhu D, Dong CX, Kriven WM, Loh R, Huang J. Ceramic Eng Sci Proc 1996;17(4):258–65.
[87] Huang CM, Zhu D, Cong X, Kriven WM, Loh RR, Huang J. J Am Ceram Soc 1997;80(9):2326–32.
[88] Kim T-J, Park C-K. Cem Concr Res 1998;28(7):955–60.
[89] Igarashi S, Kawamura M. Doboku Gakkai Rombun-Hokokushu/Proc Japan Soc Civil Eng, vol. 502, pt 5–25, 1994:83–92.
[90] Bayasi MZ, Zeng J. ACI Struct J 1997;94(4):442–6.
[91] Campione G, Mindess S, Zingone G. ACI Mater J 1999;96(1):27–34.
[92] Yamada T, Yamada K, Kubomura K. J Composite Mater 1995;29(2):179–94.
[93] Delvasto S, Naaman AE, Throne JL. Int J Cement Composites Lightweight Concrete 1986;8(3):181–90.
[94] Park C. Nippon Seramikkusu Kyokai. Gakujutsu Ronbunshi—J Ceramic Soc Jpn 1998;106(1231):268–71.
[95] Shao Y, Marikunte S, Shah SP. Concrete Int 1995;17(4):48–52.
[96] Ohama Y. Carbon 1989;27(5):729–37.
[97] Inagaki M. Carbon 1991;29(3):287–95.
[98] Lin S-S. SAMPE J 1994;30(5):39–45.
[99] Zheng Z, Feldman D. Progr Polym Sci 1995;20(2):185–210.
[100] Banthia N. Indian Concrete J 1996;70(10):533–42.
[101] Kucharska L, Brandt AM. Arch Civil Engng 1997;43(2):165–87.
[102] Pangrazzi R, Hartt WH, Kessler R. Corrosion (Houston) 1994;50(3):186.
[103] Wen S, Chung DDL. Cem Concr Res 2000 (in press).
[104] Hou J, Chung DDL. Corrosion Sci 2000 (in press).